Article

Enhanced Hydrogen Storage Properties of Li-RHC System with In-House Synthesized AlTi₃ Nanoparticles

Thi-Thu Le [1], Claudio Pistidda [1,*], Julián Puszkiel [1,2], María Victoria Castro Riglos [3], David Michael Dreistadt [1], Thomas Klassen [1,2] and Martin Dornheim [1,*]
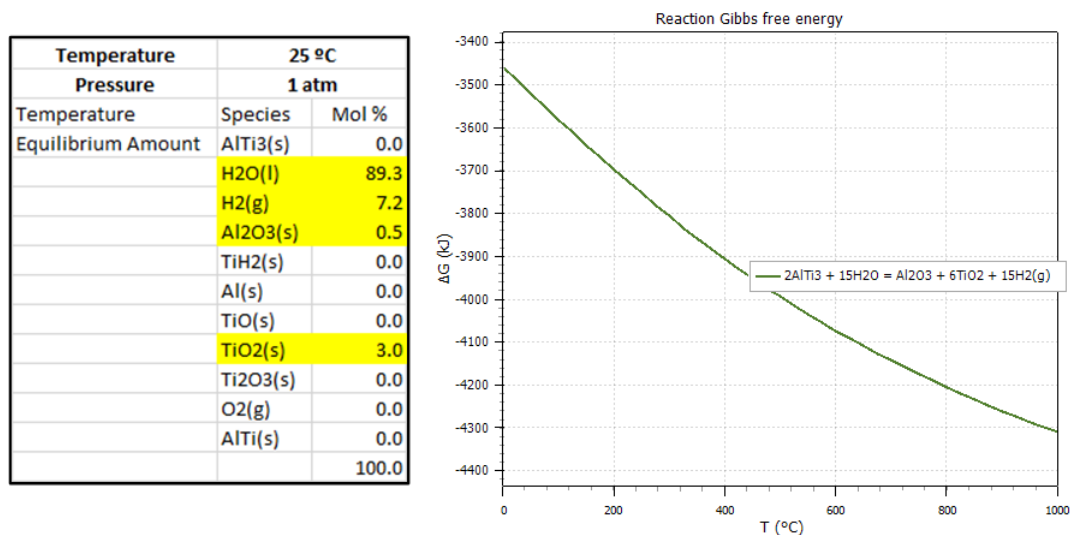
Figure S1. Gibbs minimization equilibrium calculations for the interaction between AlTi₃ and water.

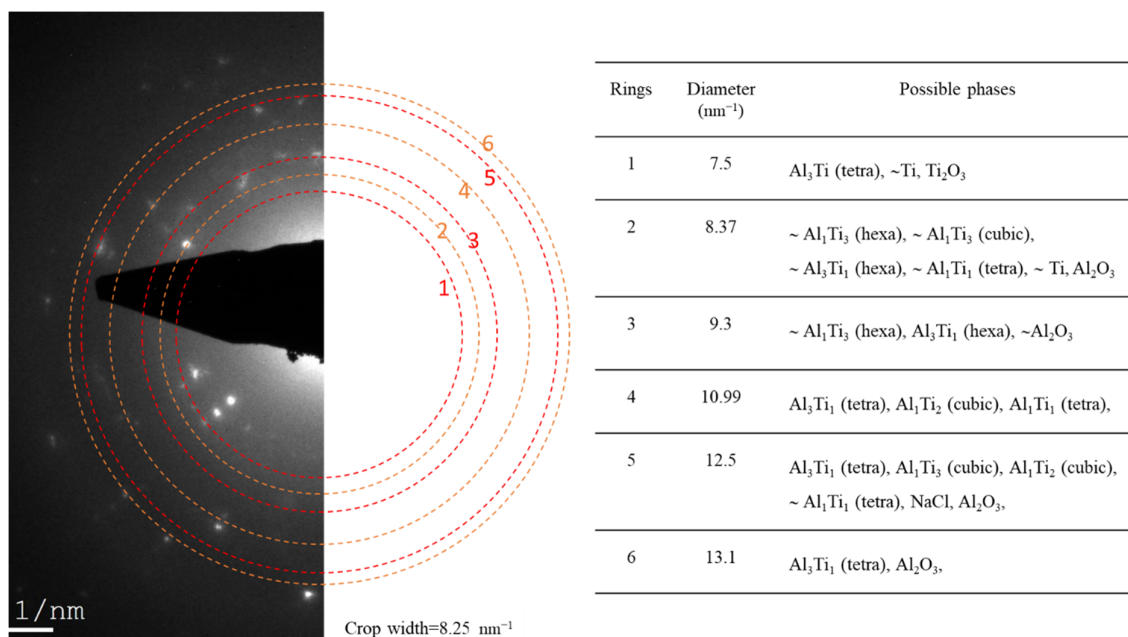| Rings	Diameter (nm⁻¹)	Possible phases
1	7.5	Al_3Ti (tetra), ~Ti, Ti_2O_3
2	8.37	~ Al_1Ti_3 (hexa), ~ Al_1Ti_3 (cubic), ~ Al_3Ti_1 (hexa), ~ Al_1Ti_1 (tetra), ~ Ti, Al_2O_3
3	9.3	~ Al_1Ti_3 (hexa), Al_3Ti_1 (hexa), ~Al_2O_3
4	10.99	Al_3Ti_1 (tetra), Al_1Ti_2 (cubic), Al_1Ti_1 (tetra),
5	12.5	Al_3Ti_1 (tetra), Al_1Ti_3 (cubic), Al_1Ti_2 (cubic), ~ Al_1Ti_1 (tetra), NaCl, Al_2O_3,
6	13.1	Al_3Ti_1 (tetra), Al_2O_3,

Figure S2. TEM diffraction of the mixture NaH + 3TiCl₃·AlCl₃ after washing and drying and possible phases.

Table S1. Interplanar spacing mismatch (%) of possible close-packed plane pair between MgB_2 (ICSD 94255), $AlTi_3$ (ICSD 58188) and Al_2O_3 (ICSD 73724).

Matching. pairs	$\{10\bar{1}1\}_{MgB_2}//$ $\{20\bar{2}1\}_{AlTi_3}$	$\{10\bar{1}1\}_{MgB_2}//$ $\{20\bar{2}2\}_{AlTi_3}$	$\{10\bar{1}1\}_{MgB_2}//$ $\{20\bar{2}0\}_{AlTi_3}$	$\{10\bar{1}0\}_{MgB_2}//$ $\{20\bar{2}1\}_{AlTi_3}$	$\{10\bar{1}0\}_{MgB_2}//$ $\{20\bar{2}2\}_{AlTi_3}$	$\{10\bar{1}0\}_{MgB_2}//$ $\{20\bar{2}0\}_{AlTi_3}$	$\{0002\}_{MgB_2}//$ $\{20\bar{2}1\}_{AlTi_3}$
f_d	3.53	−20	17.6	17.5	−36.3	−6.3	27.6

	$\{0002\}_{MgB_2}//$ $\{20\bar{2}2\}_{AlTi_3}$	$\{0002\}_{MgB_2}//$ $\{20\bar{2}0\}_{AlTi_3}$	$\{10\bar{1}1\}_{MgB_2}//$ $\{11\bar{2}0\}_{Al_2O_3}$	$\{10\bar{1}0\}_{MgB_2}//$ $\{11\bar{2}0\}_{Al_2O_3}$	$\{0002\}_{MgB_2}//$ $\{11\bar{2}0\}_{Al_2O_3}$		
f_d	3.33	42.2	17.6	−11.1	35.1		

Table S2. Interatomic spacing misfit (%) of possible matching directions between MgB_2 (a = 3.085 Å, c = 3.521 Å), $AlTi_3$ (a = 5.78 Å, c = 4.647 Å) and Al_2O_3 (a = 4.754 Å, c = 12.982 Å).

Matching pairs	$\langle 11\bar{2}0\rangle_{MgB_2}//$ $\langle 11\bar{2}0\rangle_{AlTi_3}$	$\langle 11\bar{2}3\rangle_{MgB_2}//$ $\langle 10\bar{1}0\rangle_{AlTi_3}$	$\langle 11\bar{2}3\rangle_{MgB_2}//$ $\langle 11\bar{2}3\rangle_{AlTi_3}$	$\langle 11\bar{2}3\rangle_{MgB_2}//$ $\langle 0001\rangle_{AlTi_3}$	$\langle 10\bar{1}0\rangle_{MgB_2}//$ $\langle 10\bar{1}0\rangle_{AlTi_3}$	$\langle 10\bar{1}0\rangle_{MgB_2}//$ $\langle 11\bar{2}3\rangle_{AlTi_3}$
f_s	46.6	19	58.4	−0.73	36.9	58.4

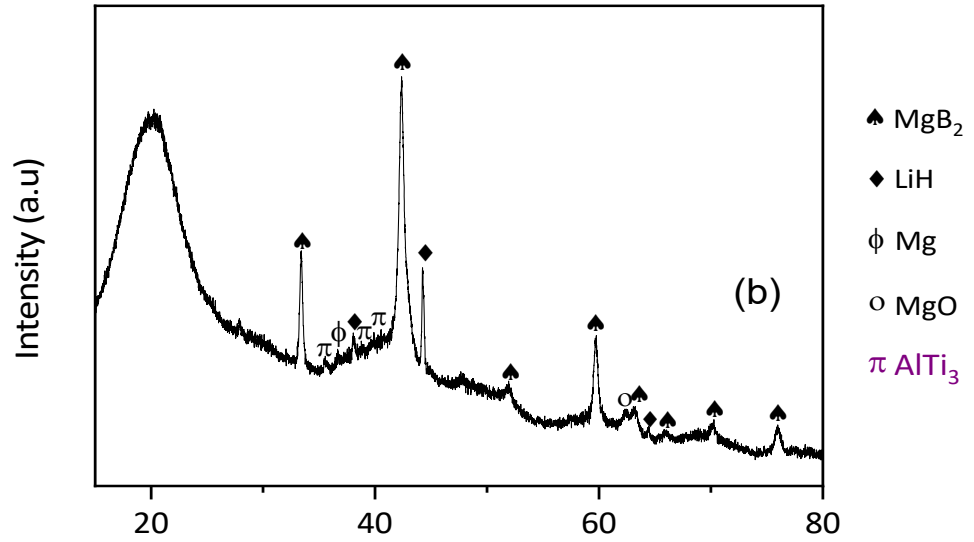|	$\langle 10\bar{1}0\rangle_{MgB_2}//$ $\langle 0001\rangle_{AlTi_3}$	$\langle 0001\rangle_{MgB_2}//$ $\langle 10\bar{1}0\rangle_{AlTi_3}$	$\langle 0001\rangle_{MgB_2}//$ $\langle 11\bar{2}3\rangle_{AlTi_3}$	$\langle 0001\rangle_{MgB_2}//$ $\langle 0001\rangle_{AlTi_3}$	$\langle 11\bar{2}0\rangle_{MgB_2}//$ $\langle 10\bar{1}0\rangle_{Al_2O_3}$	
f_s	33.6	39.1	52.5	24.2	35.1	

Figure S3. XRD diffractograms of Li-RHC + $AlTi_3$ sample after 4 cycles.

Table S3. Gas-solid reaction models and their integral expressions [36,68].

Kinetic models		Description	Integral form $g(\alpha) = k \times t$	Rate equations to be used for Sharp and Jone's method $(t/t0.5)$
Nucleation and growth models	Johnson-Mehl-Avrami (JMA, n = 1)	One-dimensional growth with interface-controlled reaction rate	$[-\ln(1-\alpha)^{1/n}]$	$[\frac{-\ln(1-\alpha)}{0.6931}]$
	Johnson-Mehl-Avrami (JMA, n = 2)	Two-dimensional growth of the existent nuclei at constant interface rate		$[\frac{-\ln(1-\alpha)^{1/2}}{0.832}]$
	Johnson-Mehl-Avrami (JMA, n = 3)	Three-dimensional growth of random nuclei with decreasing interface rate, diffusion-controlled		$[\frac{-\ln(1-\alpha)^{1/3}}{8849}]$
Diffusion models	1-D Diffusion	Surface controlled (Chemisorption)	α^2	$\frac{\alpha^2}{0.25}$
	2-D Diffusion	Two-dimensional diffusion-controlled growth with decreasing interface rate	$(1-\alpha)\ln(1-\alpha)+\alpha$	$\frac{(1-\alpha)\ln(1-\alpha)+\alpha}{0.1534}$
	3-D Diffusion	Three-dimensional diffusion-controlled growth with decreasing interface rate	$1-\frac{2}{3}\alpha-(1-\alpha)^{2/3}$	$\frac{1-\frac{2}{3}\alpha-(1-\alpha)^{2/3}}{0.04255}$
Geometrical contracting models	Contracting area (CA), n = 2	Two-dimensional growth of contracting volume with constant interface rate	$1-(1-\alpha)^{1/n}$	$\frac{1-(1-\alpha)^{1/2}}{0.29289}$
	Contracting volume (CV), n = 3	Three-dimensional growth of contracting volume with constant interface rate		$\frac{1-(1-\alpha)^{1/3}}{0.20629}$

Table S4. Fitting parameters of the hydrogenation kinetic curves.

Fitting model: CV (n = 3) $f(\alpha) = 1 - (1 - k \times t)^3$			
T (°C)	k	Sdt. Error	Adj. R-Square
380	0.0003242	$3.09372 \cdot 10^{-6}$	0.9895
390	0.0004456	$3.75844 \cdot 10^{-6}$	0.9911
400	0.0006388	$6.53853 \cdot 10^{-6}$	0.9899
410	0.0008238	$1.06936 \cdot 10^{-5}$	0.99877

Table S5. Fitting parameters of the dehydrogenation kinetic curves.

Fitting model: JMA (n=1) + Modified Prout Topkins $f(\alpha) = A_1 \times (1 - \exp(-k_1 \times t)) + A_2 \times (1 + exp[-(k_2 \times (t - t_0))]^m)$ [50]							
		First step			Second step		
T (°C)	R^2	A_1	k_1	n	A_2	k_2	t_0
370	0.9998	0.28279635	0.00529	1	0.81832835	$1.08591 \cdot 10^{-4}$	$4.32318 \cdot 10^4$
380	0.9999	0.26640137	0.00756	1	0.75455501	$2.73158 \cdot 10^{-4}$	$1.58231 \cdot 10^4$
390	0.9992	0.28851172	0.01162	1	0.79827248	$5.51551 \cdot 10^{-4}$	$6.98715 \cdot 10^3$
400	0.9993	0.27015373	0.01841	1	0.85972961	0.001045	$3.56581 \cdot 10^3$